Computer Assisted Methods in Engineering and Science
30(4): 521–537, 2023, doi: 10.24423/cames.1015

Identification of Thermophysical Parameters Using an Artificial Immune System

Jolanta DZIATKIEWICZ, Arkadiusz POTERALSKI*

Department of Computational Mechanics and Engineering, Silesian University of Technology, Gliwice, Poland; e-mail: jolanta.dziatkiewicz@polsl.pl

** Corresponding Author e-mail: arkadiusz.poteralski@polsl.pl*

In this paper, the identification of thermophysical parameters using the hyperbolic two-temperature model is made. We investigate the influence of ultra-fast laser pulses on the heating of a thin metal film using this model. Two differential equations coupled with the electron-phonon coupling factor G are used. One of these equations concerns electron temperatures and the other addresses lattice temperatures. Appropriate initial and boundary conditions are imposed for this model. The finite difference method with a staggered grid is used to solve this direct problem. Temperatures for even nodes and heat fluxes for odd nodes are calculated. The results of the direct problem and results of the experiment are compared. In the optimization process, an artificial immune system is used.

Keywords: microscale heat transfer, two-temperature model, final difference method, artificial immune system.

1. Introduction

The optimization of mechanical structures is very difficult and requires a lot of time to solve a given problem [5]. It involves solving multiple direct problems that can be very complex and then calculating fitness function value and sometimes its gradient. During the optimization process, using one of effective optimization methods, for example, an artificial immune system (AIS), is of great importance. The application of this method in conjunction with the finite element method (FEM), the finite difference method (FDM) or the boundary element method (BEM) enables the optimization of mechanical structures. The biological immune systems were the inspiration to create the AIS [28]. Three different mechanisms of immune system can be employed: positive and negative and mechanism of clonal selection used in this paper. The AIS optimization al-

gorithm has been used extensively to optimize a variety of mechanical structures, including shell structures and solid shell structures. The optimization concerned changes in shape, topology and material properties [29]. Other examples of using this approach include optimizing: elastic vibrating systems [31], magneto-electric composites [34] thermomechanical structures [36], and porous structure parameters [35]. Additionally, it has also been employed in the identification processes, such as determining parameters of composites structures [30], addressing acoustics problem [32], and identifying material constants for piezoelectric materials [33].

Based on many numerical examples, we can conclude that AIS provides a good probability of finding the global optimum and helps avoiding local solutions. The primary purpose of immune algorithms is to improve efficiency and effectiveness during the identification and optimization process. The modification (hybridization) of the classical AIS can be used to improve the optimization process [11]. There are two types of modification to consider. First type of modification concerns the use of hypermutation gradient, while the other is based on the Kriging method [19]. The goal of these two new optimization algorithms is to reduce the time required and ensure a better convergence to the global optimum. The advantage of the second type of modification is its applicability to uncertainty problem [33].

The efficiency and effectiveness of the optimization process using an immune algorithm depend on the proper configuration of its parameters. During each optimization or identification process, the parameters of this algorithm are tested, and the optimal values determined through these tests are used. Setting wrong values for these parameters can lead to reduced efficiency and effectiveness in the optimization process. Additionally, the local solutions can be found when using the wrong parameter values, limiting the ability to find the global optimal solution.

In the past, the AIS algorithms [6] were employed in many different problems. For example, the AIS approach was used in a multi-objective optimization [7, 15], neural network learning [9, 22, 23], and query expansion problem [8]. Furthermore, the AIS have also many interesting applications not related to mechanics, for example, reconstructing phylogenetic trees [15] or diagnosing heart diseases based on ECG analysis [3]. Other interesting examples include controlling and identifying a fuel-ethanol fermentation process and optimal selection of Wiener equalizers [2]. In several articles, we can also find modifications of the classic AIS: Bayesian AIS (BAIS) [10, 12]. Other examples include optimization in transportation systems [20, 22] and another method of hybridization [18].

In this paper, the identification of thermophysical parameters of thin metal film subjected to laser pulses is conducted. The hyperbolic two-temperature model is employed for this purpose. This two-temperature model is described in

two differential equations coupled with the electron-phonon coupling factor G. One equation concerns electron temperatures and the other addresses lattice temperatures [14, 38]. Appropriate initial and boundary conditions were imposed for this model. The FDM with a staggered grid was employed to solve this direct problem [21, 24]. Temperatures for even nodes and heat fluxes for odd nodes were calculated. The results of the direct problem were next compared with experimental data.

In summary, various versions of AIS have been employed during many identification or optimization problems for a wide range of engineering problems.

It is important to note that the problem described in this article has not yet been solved using the AIS approach. In this article, the following issues are described. In Sec. 2, microscale heat transfer for the two-temperature model is presented. The direct problem is formulated in Sec. 3. In Sec. 4, the principle of AIS operation is described and explained. In Sec. 5, the optimization problem and numerical example are presented. Concluding remarks are given in Sec. 6.

2. Heat transfer in microscale – two-temperature model

In the paper, a thin metal film is considered. The thickness of this film is L. Because the laser spot size is larger than the thickness of the film [1, 14], the problem is treated as a one-dimensional (1D). At the left boundary, where $x = 0$, the film is irradiated by an ultrashort laser pulse (Fig. 1). The equations below describe the temporal and spatial distribution of lattice and electron temperatures in the thin irradiated film [26]

$$C_e(T_e)\frac{\partial T_e(x,t)}{\partial t} = -\frac{\partial q_e(x,t)}{\partial x} - G[T_e(x,t) - T_l(x,t)] + Q(x,t) \tag{1}$$

and

$$C_l\frac{\partial T_l(x,t)}{\partial t} = -\frac{\partial q_l(x,t)}{\partial x} + G[T_e(x,t) - T_l(x,t)], \tag{2}$$

where $C_e(T_e)$ is the volumetric specific heat of electrons, C_l is the volumetric specific heat of lattice, G is the electron-phonon coupling factor that represents

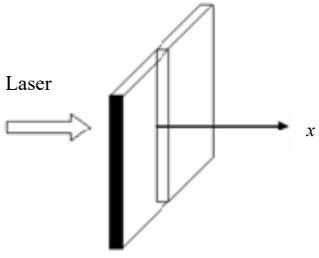

Fig. 1. Laser heating of the thin metal film.

the energy exchange between electrons and lattice, $q_e(x,t)$ and $q_l(x,t)$ are the heat fluxes, and $Q(x,t)$ is the source connected with the laser pulse.

In micro heat transfer, the classical Fourier law is replaced by the following formulas:

$$q_e(x,t) + \tau_e \frac{\partial q_e(x,t)}{\partial t} = -\lambda_e(T_e, T_l) \frac{\partial T_e(x,t)}{\partial x} \tag{3}$$

and

$$q_l(x,t) + \tau_l \frac{\partial q_l(x,t)}{\partial t} = -\lambda_l \frac{\partial T_l(x,t)}{\partial x}, \tag{4}$$

where $\lambda_e(T_e, T_l)$ is the thermal conductivity of the electrons, λ_l is the thermal conductivity of the lattice, τ_e is the time required to change energy state of electrons called relaxation time of free electrons, and τ_l is the relaxation time in phonon collisions. The heat source $Q(x,t)$ is given as [14, 25]:

$$Q(x,t) = \sqrt{\frac{\beta}{\pi}} \frac{1-R}{t_p \delta} I_0 \exp\left[-\frac{x}{\delta} - \beta \frac{(t-2t_p)^2}{t_p^2}\right], \tag{5}$$

where t_p is the characteristic time of laser pulse, I_0 is the laser intensity, δ is the optical penetration depth, R is the reflectivity of the irradiated surface, and $\beta = 4 \ln 2$.

The laser heating takes the ultrashort period of time so the heat losses from boundary surfaces of thin metal film can be neglected [14, 17], and this means

$$q_e(0,t) = q_e(L,t) = q_l(0,t) = q_l(L,t) = 0, \tag{6}$$

where L is the thickness of the thin film. The initial conditions are as follows:

$$t = 0 \; : \quad T_e(x,0) = T_l(x,0) = T_p. \tag{7}$$

The formulas for the thermal conductivity λ_e and heat capacity C_e of electrons are given [14, 24]:

$$\lambda_e(T_e, T_l) = \lambda_0 \frac{T_e}{T_l} \tag{8}$$

and

$$C_e(T_e) = \gamma T_e, \tag{9}$$

where λ_0, γ are the material constants. It needs to be highlighted that the simple form of expressions (8) and (9) is only suitable for temperatures T_e much more smaller than the Fermi temperature $T_F = E_F/k_B$, where E_F, k_B are the Fermi energy and Boltzmann constant, respectively [24].

3. The direct problem – solution method

To solve the direct problem, the FDM is employed. Specifically, the version of this method with staggered grid (Fig. 2) [16, 27] is applied. This means that even nodes are introduced: $T_{ei}^{f} = T_e(ih,\ f\Delta t)$, $T_{li}^{f} = T_l(ih, f\Delta t)$, where h is the mesh size, Δt is the time step, and $i = 0, 2, 4, ..., N$, $f = 0, 1, 2, ..., F$. For odd nodes, we introduce $q_{ej}^{f} = q_e(jh, f\Delta t)$, $q_{lj}^{f} = q_l(jh, f\Delta t)$, where $j = 1, 3, ..., N-1$.

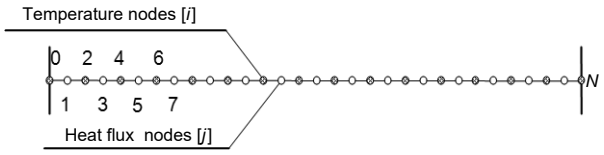

Fig. 2. Discretization for 1D model.

An explicit scheme of the FDM is formulated. Approximation of Eqs. (4) and (5) can be written in the form:

$$q_{ej}^{f-1} + \tau_e \frac{q_{ej}^{f} - q_{ej}^{f-1}}{\Delta t} = -\lambda_{ej}^{f-1} \frac{T_{ej+1}^{f-1} - T_{ej-1}^{f-1}}{2h} \tag{10}$$

and

$$q_{lj}^{f-1} + \tau_l \frac{q_{lj}^{f} - q_{lj}^{f-1}}{\Delta t} = -\lambda_l \frac{T_{lj+1}^{f-1} - T_{lj-1}^{f-1}}{2h}, \tag{11}$$

where the index j corresponds to the odd nodes – heat flux nodes (Fig. 2).

Equations (1) and (2) are also discretized and written in the form:

$$C_{ei}^{f-1} \frac{T_{ei}^{f} - T_{ei}^{f-1}}{\Delta t} = -\frac{q_{ei+1}^{f} - q_{ei-1}^{f}}{2h} - G\left(T_{ei}^{f-1} - T_{li}^{f-1}\right) + Q_i^{f-1} \tag{12}$$

and

$$C_l \frac{T_{li}^{f} - T_{li}^{f-1}}{\Delta t} = -\frac{q_{li+1}^{f} - q_{li-1}^{f}}{2h} + G\left(T_{ei}^{f-1} - T_{li}^{f-1}\right), \tag{13}$$

where the index i corresponds to the even nodes – temperature nodes, as shown in Fig. 2.

The modification of the heat fluxes from the odd nodes to the even nodes is as follows:

$$q_{ei-1}^{f} - q_{ei+1}^{f} = \frac{\tau_e - \Delta t}{\tau_e}\left(q_{ei-1}^{f-1} - q_{ei+1}^{f-1}\right) + \frac{\Delta t}{2h\tau_e}\left[\lambda_{ei-1}^{f-1}\left(T_{ei-2}^{f-1} - T_{ei}^{f-1}\right) + \lambda_{ei+1}^{f-1}\left(T_{ei+2}^{f-1} - T_{ei}^{f-1}\right)\right] \tag{14}$$

and

$$q_{li-1}^{f} - q_{li+1}^{f} = \frac{\tau_l - \Delta t}{\tau_l}\left(q_{li-1}^{f-1} - q_{li+1}^{f-1}\right) + \frac{\lambda_l \Delta t}{2h\tau_l}\left(T_{li-2}^{f-1} - 2T_{li}^{f-1} + T_{li+2}^{f-1}\right). \quad (15)$$

By putting (14) into (12) and (16) into (13), one obtains:

$$C_{ei}^{f-1}\frac{T_{ei}^{f} - T_{ei}^{f-1}}{\Delta t} = \frac{(\tau_e - \Delta t)}{2h\tau_e}\left(q_{ei-1}^{f-1} - q_{ei+1}^{f-1}\right) + \frac{\Delta t}{4h^2\tau_e}\left[\lambda_{ei-1}^{f-1}\left(T_{ei-2}^{f-1} - T_{ei}^{f-1}\right) + \lambda_{ei+1}^{f-1}\left(T_{ei+2}^{f-1} - T_{ei}^{f-1}\right)\right] - G\left(T_{ei}^{f-1} - T_{li}^{f-1}\right) + Q_i^{f-1} \quad (16)$$

and

$$C_l\frac{T_{li}^{f} - T_{li}^{f-1}}{\Delta t} = \frac{(\tau_l - \Delta t)}{2h\tau_l}(q_{li-1}^{f-1} - q_{li+1}^{f-1}) + \frac{\lambda_l \Delta t}{4h^2\tau_l}(T_{li-2}^{f-1} - 2T_{li}^{f-1} + T_{li+2}^{f-1}) + G\left(T_{ei}^{f-1} - T_{li}^{f-1}\right). \quad (17)$$

After mathematical transformations based on Eqs. (16) and (17), we obtain:

$$T_{ei}^{f} = \left(1 - A_{ei}^{f-1} - B_{ei}^{f-1} - \frac{G\Delta t}{C_{ei}^{f-1}}\right)T_{ei}^{f-1} + A_{ei}^{f-1}T_{ei-2}^{f-1} + B_{ei}^{f-1}T_{ei+2}^{f-1} + \frac{G\Delta t}{C_{ei}^{f-1}}T_{li}^{f-1} + \frac{\Delta t(\tau_e - \Delta t)}{2h\tau_e C_{ei}^{f-1}}\left(q_{ei-1}^{f-1} - q_{ei+1}^{f-1}\right) + \frac{Q_i^{f-1}\Delta t}{C_{ei}^{f-1}} \quad (18)$$

and

$$T_{li}^{f} = \left(1 - 2A_{li}^{f-1} - \frac{G\Delta t}{C_l}\right)T_{li}^{f-1} + A_{li}^{f-1}\left(T_{li-2}^{f-1} + T_{li+2}^{f-1}\right) + \frac{G\Delta t}{C_l}T_{ei}^{f-1} + \frac{\Delta t(\tau_l - \Delta t)}{2h\tau_l C_l}\left(q_{li-1}^{f-1} - q_{li+1}^{f-1}\right), \quad (19)$$

where:

$$A_{ei}^{f-1} = \frac{(\Delta t)^2(\lambda_{ei-2}^{f-1} + \lambda_{ei}^{f-1})}{8h^2\tau_e C_{ei}^{f-1}}, \qquad B_{ei}^{f-1} = \frac{(\Delta t)^2(\lambda_{ei}^{f-1} + \lambda_{ei+2}^{f-1})}{8h^2\tau_e C_{ei}^{f-1}}, \quad (20)$$

$$A_{li}^{f-1} = \frac{\lambda_l(\Delta t)^2}{4h^2\tau_l C_l}. \quad (21)$$

The thermal conductivities are also approximated as follows:

$$\lambda_{ej}^{f-1} = \frac{\lambda_{ej-1}^{f-1} + \lambda_{ej+1}^{f-1}}{2}. \tag{22}$$

The stability criteria for the explicit scheme of the FDM are formulated (Eqs. (10) and (11)):

$$\frac{\tau_e - \Delta t}{\tau_e} \geq 0, \qquad \frac{\tau_l - \Delta t}{\tau_l} \geq 0 \tag{23}$$

and (Eqs. (18) and (19)):

$$1 - A_{ei}^{f-1} - B_{ei}^{f-1} - \frac{G\Delta t}{C_{ei}^{f-1}} \geq 0, \qquad 1 - 2A_{li}^{f-1} - \frac{G\Delta t}{C_l} \geq 0. \tag{24}$$

For the transition $t^{f-1} \to t^f$, Eqs. (10) and (11) are solved first and then the temperatures T_e and T_l are defined using Eqs. (18) and (19).

4. Optimization algorithm – AIS

Three different mechanisms of AIS can be used: positive, negative and clonal selection mechanism used in this paper [4, 13]. This AIS approach is presented in Fig. 3. It works in several stages. In the first stage, memory cells are randomly generated. In the next stage, new memory cells are generated using a procedure of proliferation and mutations. The number of clones created for each memory cell depends on the value of the objective function for a considered memory cell. In the subsequent stage, the value of the objective function is calculated for each memory cell and its clones. Selection is the next stage of AIS. During this process,

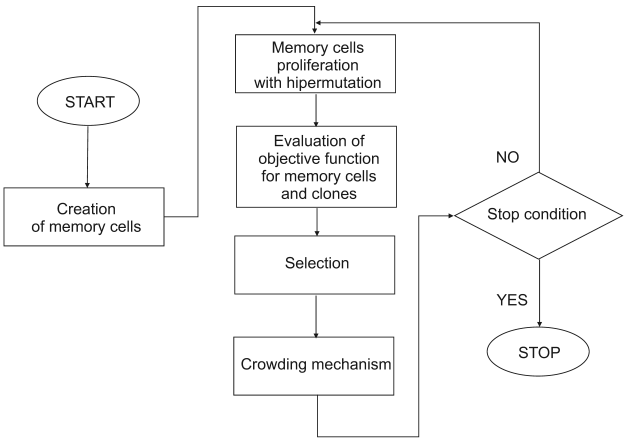

Fig. 3. Artificial immune system.

memory cells are compared with their clones and the clones with the better value of objective function replace the original memory cells. The next and very important stage ensuring diversity of the population of solutions is crowding mechanism. During this stage, similar memory cells are eliminated. The whole optimization process is performed iteratively until the stop condition is met.

Several different stop conditions can be used, such as the maximum number of iterations, a target value for the objective function and expected improvement in the objective function after several iterations. This type of AIS is based on the Wierzchoń method [37]. The difference between Wierzchoń's method and the method described in this article is the use of a different mutation operator. In this study, a Gaussian mutation is employed instead of the nonuniform mutation [37].

For the optimization problem, an objective function is defined. During the immune optimization, the objective function is minimized (or maximized) J:

$$\min_{\mathbf{x}} J(\mathbf{x}) \tag{25}$$

for the decision variables, which are described in following form:

$$\mathbf{x}_t^j = \left[g_1^j, g_2^j, ..., g_i^j, ..., g_n^j\right], \tag{26}$$

where g_i^j is the i-th parameter of j-th vector, i.e., the decision variable during the optimization problem, and t is the iteration number.

The optimization process of any structure often involves equality or inequality constraints. These constraints are imposed on the parameters of the vector (decision variables) from Eq. (26):

$$g_{i\,\min}^j \leq g_i^j \leq g_{i\,\max}^j, \tag{27}$$

where $g_{i\,\min}^j$ is the minimum value of the decision variable for the j-th memory cell, and $g_{i\,\max}^j$ is the maximum value of the decision variable for the j-th memory cell.

At the beginning of immunology process, memory cells are generated. The parameter L_{kp} describes the number of memory cells in each iteration. During the optimization process, the memory cells that contain decision variables are proliferated. This process involves creating clones based on memory cells. All memory cells and their clones form the population for which objective functions are calculated. The parameter L_{pop_kl} describes the number of clones in each iteration, and the parameter L_{pop} describes the size of the entire population (memory cells and their clones). Proliferation of memory cells occurs in the main loop of immune process (the first stage of immune algorithm). The declared number of clones is generated for each memory cell. The declared number of

clones is generated for the best memory cell (parameter L_{kl}). For other memory cells, only half of the declared number of clones is generated.

The population of all cells is expressed by the following equations:

$$L_{pop} = L_{kp} + L_{pop\_kl}, \tag{28}$$

$$L_{pop\_kl} = L_{kl} + (L_{kp} - 1)\,\frac{L_{kl}}{2}, \tag{29}$$

where L_{kp} is the number of memory cells in each iteration, L_{kl} is the number of clones in each iteration, L_{pop} is the size of the entire population (memory cells and their clones), and L_{pop_kl} is the population of clones in each iteration.

In this immune algorithm, the mechanism of hypermutation is used. The main purpose of this operator is the formation of new, modified (differentiated) memory cells. The probabilistic method of modifying a randomly selected fragment of the memory cell is used. Each position of memory cell is mutated with certain probability $\mathrm{mut_G}$, using this modification:

$$g^j_{i\_\mathrm{new}} = g^j_i + \Delta g^j_i, \qquad i = 1, ..., L_{pop\_kl}, \tag{30}$$

where $g^j_{i\_\mathrm{new}}$ is the new value of memory cell parameter (using the modification of Gaussian mutation), g^j_i is the i-th parameter of the j-th memory cell (i-th decision variable during the optimization process), and Δg^j_i is a variable corresponding to the application of Gaussian mutation.

The value of objective function is calculated for all memory cells and their modified clones. Then, the selection process is performed. During this procedure, less effective memory cells are replaced with more efficient clones. Finally, some old memory cells (from previous iteration) are replaced by better memory cells. This selection mechanism is illustrated in Fig. 4. The selection mechanism is based on the following idea with two memory cells MC-A and MC-B. For each of these memory cells, four respective clones, named from C-A1 to C-A4 and C-B1 to C-B4, are created. Next, the objective function of each memory cell is compared with the objective function of its clones. After this comparison, clone C-A4 and memory cell MC-B are selected for the next iteration. This operation is repeated for each memory cell.

Next and important stage of immune process is the crowding mechanism. This procedure ensures the maintenance of diversity within the population of memory cells. During this procedure, similar memory cells are deleted. The similarity is determined as the geometrical distance between two memory cells (Fig. 5). The parameter $\mathrm{min_{dis}}$ defines this minimal distance. The crowding mechanism is illustrated in Fig. 5. During this mechanism, two memory cells are compared. In Fig. 5, only memory cells 1 and 2 are in the similarity region and the better

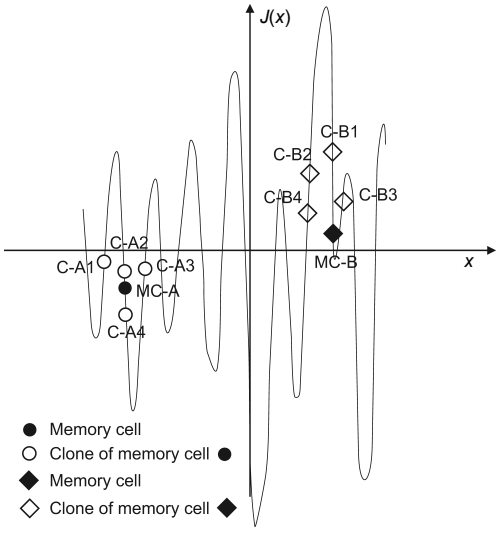

FIG. 4. Graphical representation of the selection mechanism.

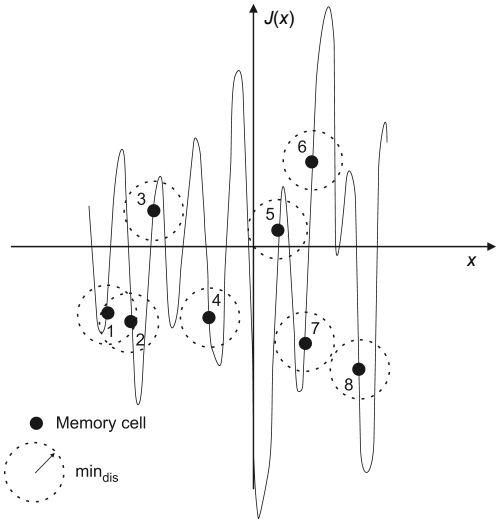

FIG. 5. Graphical representation of the crowding mechanism.

one remains in the population and the worse is eliminated. After eliminating the inferior memory cell, a new memory cell is generated randomly.

The minimum distance between two points for the crowding mechanism $\min_{\text{dis}}$ is:

$$\min{}_{\text{dis}} = 0.1 \min{}_{\text{dom}} \left(\sqrt{\sum_{i=1}^{n} (g_{i\,\max}^{j} - g_{i\,\min}^{j})^2} \right), \tag{31}$$

where $g^j_{i\,\min}$ is the i-th minimum value of the decision variable parameter (memory cell), $g^j_{i\,\max}$ is the i-th maximal value of the decision variable parameter (memory cell), n is the number of the decision variables, and $\min_{\text{dom}}$ is a parameter deciding about the size of the search space (memory cell comparison).

The iterative optimization process is stopped after stop condition is fulfilled. The stop condition is determined as the maximum number of iterations.

5. Identification of thermophysical parameters

In the parameter identification process, a basis for experimental data is established. The main purpose of identification is to obtain a model that will reflect the actual course of the process as accurately as possible. The purpose of identification process using an AIS is to assess the values of thermophysical parameters. These parameters occur in a hyperbolic two-temperature model in which the thin metal film was heated by laser pulses. The results of experiment are compared with the results of the direct problem.

For this purpose, an optimization problem is formulated and solved using an AIS. The value of the objective function determines the quality of the obtained solution. The objective function is based on the least squares method or the norm between the values derived from the numerical model and the experimental measurements. The objective function has the following form:

$$J(\mathbf{x}) = \sqrt{\frac{\sum_{i=1}^{n} \left(d_i(\mathbf{x}) - d_{i_{\text{ref}}}\right)^2}{n}}, \tag{32}$$

where $\mathbf{x}$ is the vector of the design variables, n is the number of sensor points measurements, $d_{i_{\text{ref}}}$ is the i-th measurement value, and $d_i(\mathbf{x})$ is the i-th value obtained from the numerical model.

For the direct problem, a layer (made of gold) with a thickness of $L = 100$ nm and the temperature at the beginning of the process $T_p = 300$ K is considered. A laser with an intensity of $I_0 = 13.4$ J/m^2 and impulse $t_p = 100$ fs is employed. For gold, a reflection coefficient is $R = 0.93$ and an optical penetration depth $\delta = 15.3$ nm [27].

Due to the relatively low laser intensity, the linear dependence of the heat capacity of electrons on their temperature: $C_e = \gamma T_e$ (formula (9)), where $\gamma = 62.9$ J/(m$^3 \cdot$K^2). The other parameters are the heat capacity of phonons: $C_l = 2.5$ MJ/(m$^3 \cdot$K), the heat conduction coefficients for phonons: $\lambda_l = \lambda_0$ and for electrons $\lambda_e = \lambda_0 T_e / T_l$ (see formula (8)), where $\lambda_0 = 315$ W/(m$\cdot$K).

For solving the direct problem, the FDM is used. The data for this method are as follows: $\Delta t = 0.0001$ ps and $h = 1$ nm. There are three design variables

identified: the electron-phonon coupling factor G, the relaxation time τ_e, and the relaxation time τ_l. The limits on the values of design variables are given in Table 1.

TABLE 1. The design parameters constraints.

Variable	Minimum value	Maximum value
τ_e [ps]	0.005	0.100
τ_l [ps]	0.10	1.60
G [W/(m$^3 \cdot$K)]	0.5×10^{16}	200.0×10^{16}

The purpose of this identification is to obtain three model parameters: the relaxation times τ_e and τ_l and the coupling coefficient G. The identification is carried out based on experimental data from [14]. Only electron temperatures for the experimental data are available, which are shown in Fig. 6. At the beginning of the process there is a rapid increase of temperature, followed by a slower decrease.

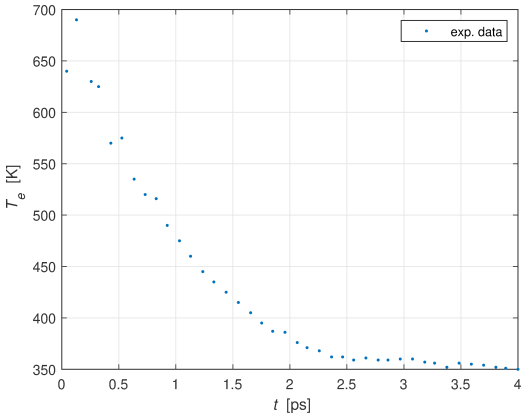

FIG. 6. Experimental data [14].

The AIS parameters are presented in Table 2.

TABLE 2. The parameters of AIS.

Numbers of decision variables	Number of memory cells	Number of the clones	Crowding factor	Gaussian mutation
3	15	15	0.5	0.5

In the first step, three variants of design variables are considered (Table 3). For the first variant, design variables are set as the minimal values of constraints,

TABLE 3. The design parameters for three variants.

Parameter	Variant 1	Variant 2	Variant 3
τ_e [ps]	0.005	0.500	0.100
τ_l [ps]	0.10	0.85	1.60
G [W/(m$^3 \cdot$K)]	0.5×10^{16}	100×10^{16}	200.0×10^{16}

for the second variant, they are average values between minimal and maximal constraint values, and for the last variant maximal values of constraints.

The results of comparing the numerical solution with the experimental solution is shown in Fig. 7. The difference between these two solutions is significant and unacceptable for all variants. The fitness function values for this three variants are: 151.18 K, 153.60 K and 152.39 K, respectively. In the next step, an AIS is used. The results of the identification process are shown in Fig. 8.

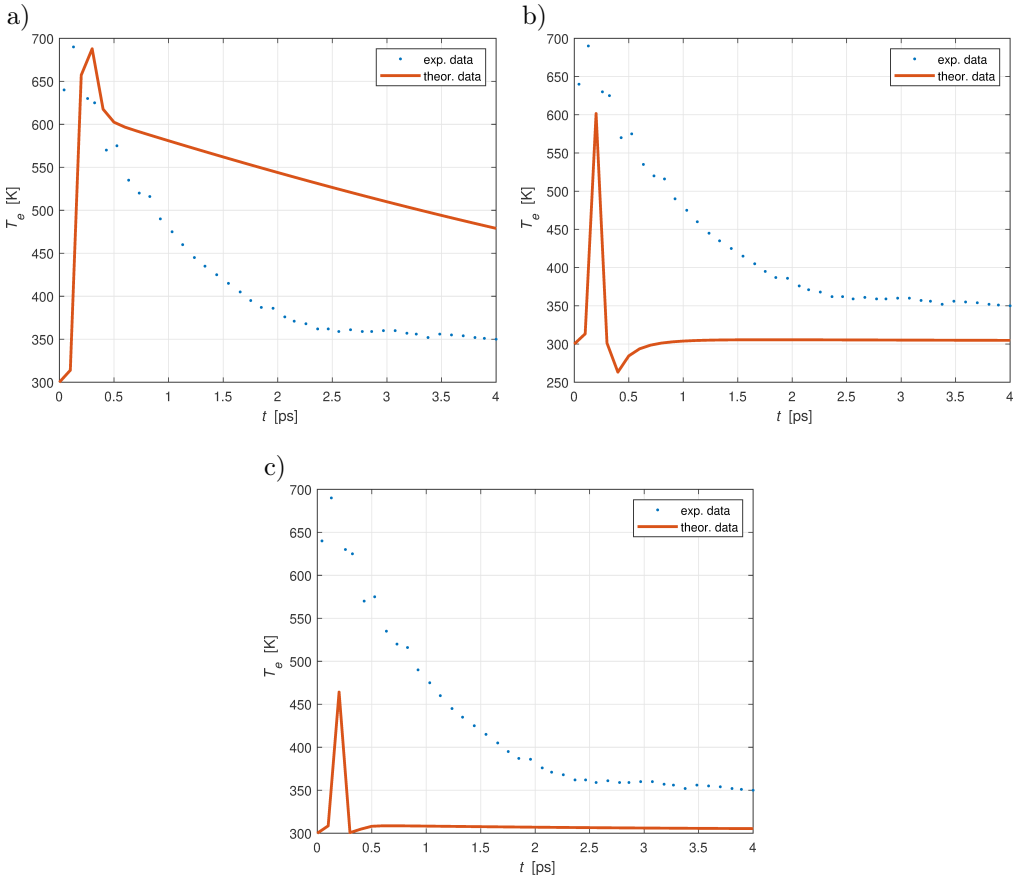

FIG. 7. The comparison of the numerical solution with the experimental solution, three variants of design parameters: a) variant 1, b) variant 2, c) variant 3.

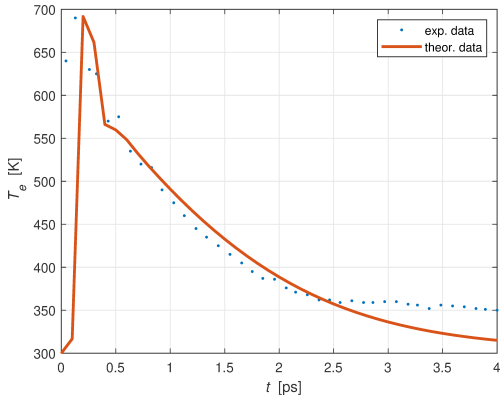

FIG. 8. Results of the identification process.

The difference between the numerical and experimental solutions is satisfactory, and the value of the objective function is 77.32 K.

6. Final conclusions

The article solved the problem of heat transfer parameters identification in a thin film subjected to a short laser pulse. An effective tool for immunological identification of thermophysical parameters was presented. The implementation of immunological algorithms in this approach gives a high probability of finding global optimal solutions. Furthermore, the presented approach can also be used to identify other material properties or initial thermal conditions and can be used for solving other problems. The effectiveness of the method can also be improved, e.g., through the use of a hybrid AIS.

References

1. M.A. Al-Nimr, Heat transfer mechanisms during short duration laser heating of thin metal films, *International Journal of Thermophysics*, **18**(5): 1257–1268, 1997, doi: 10.1007/BF02575260.

2. R.R. de Faissol Attux, M.B. Loiola, R. Suyama, L.N. de Castro, F.J. Von Zuben, J.M.T. Romano, Blind search for optimal Wiener equalizers using an artificial immune network model, *EURASIP Journal on Advances in Signal Processing*, **2003**: 460216, 2003, doi: 10.1155/S1110865703303014.

3. M. Bereta, T. Burczyński, Comparing binary and real-valued coding in hybrid immune algorithm for feature selection and classification of ECG signals, *Engineering Applications of Artificial Intelligence*, **20**(5): 571–585, 2007, doi: 10.1016/j.engappai.2006.11.004.

4. M. Bereta, T. Burczyński, Immune K-means and negative selection algorithms for data analysis, *Information Sciences*, **179**(10): 1407–1425, 2009, doi: 10.1016/j.ins.2008.10.034.

5. T. Burczynski *et al.*, Intelligent computing in evolutionary optimal shaping of solids, [in:] *Proceedings of the 3rd International Conference on Computing, Communications and Control Technologies*, Vol. 3, pp. 294–298, 2005.

6. L.N. de Castro, J. Timmis, Artificial immune systems: a novel approach to pattern recognition, [in:] J.M. Corchado, L. Alonso, C. Fyfe [Eds], *Artificial Neural Networks in Pattern Recognition*, pp. 67–84, University of Paisley, UK, 2002, https://kar.kent.ac.uk/id/eprint/13832.

7. P.A.D. Castro, F.J. Von Zuben, Multi-objective feature selection using a Bayesian artificial immune system, *International Journal of Intelligent Computing and Cybernetics*, **3**(2): 235–256, 2010, doi: 10.1108/17563781011049188.

8. P.A.D. Castro, F.O. de França, H.M. Ferreira, G.P. Coelho, F.J. Von Zuben, Query expansion using an immune-inspired biclustering algorithm, *Natural Computing*, **9**: 579–602, 2010, doi: 10.1007/s11047-009-9127-y.

9. L.N. de Castro, F.J. Von Zuben, Immune and neural network models: theoretical and empirical comparisons, *International Journal on Computational Intelligence and Applications*, **1**(3): 239–257, 2001, doi: 10.1142/S1469026801000238.

10. P.A.D. Castro, F.J. Von Zuben, BAIS: A Bayesian artificial immune system for the effective handling of building blocks, *Information Sciences*, **179**(10): 1426–1444, 2009, doi: 10.1016/j.ins.2008.11.040.

11. L.N. de Castro, F.J. Von Zuben, The construction of a Boolean competitive neural network using ideas from immunology, *Neurocomputing*, **50**: 51–85, 2003, doi: 10.1016/S0925-2312(01)00698-1.

12. P.A.D. Castro, F.J. Von Zuben, Multi-objective Bayesian artificial immune system: empirical evaluation and comparative analyses, *Journal of Mathematical Modelling and Algorithms*, **8**: 151–173, 2009, doi: 10.1007/s10852-009-9108-2.

13. L.N. de Castro, F.J. Von Zuben, Learning and optimization using the clonal selection principle, *IEEE Transactions on Evolutionary Computation, Special Issue on Artificial Immune Systems*, **6**(3): 239–251, 2002, doi: 10.1109/TEVC.2002.1011539.

14. J.K. Chen, J.E. Beraun, Numerical study of ultrashort laser pulse interactions with metal films, *Numerical Heat Transfer, Part A: Applications*, **40**(1): 1–20, 2001, doi: 10.1080/104077801300348842.

15. G.P. Coelho, A.E.A. da Silva, F.J. Von Zuben, An immune-inspired multi-objective approach to the reconstruction of phylogenetic trees, *Neural Computing & Applications*, **19**: 1103–1132, 2010, doi: 10.1007/s00521-010-0389-1.

16. J. Dziatkiewicz, W. Kuś, E. Majchrzak, T. Burczyński, Ł. Turchan, Bioinspired identification of parameters in microscale heat transfer, *International Journal for Multiscale Computational Engineering*, **12**(1): 79–89, 2014, doi: 10.1615/IntJMultCompEng.2014007963.

17. J. Dziatkiewicz, E. Majchrzak, Numerical analysis of laser ablation using the axisymmetric two-temperature model, [in:] *AIP Conference Proceedings*, vol. 1922, pp. 060004-1–060004-8, AIP Publishing, Melville, 2018, doi: 10.1063/1.5019065.

18. M. Gong, C. Liu, L. Jiao, G. Cheng, Hybrid immune algorithm with Lamarckian local search for multi-objective optimization, *Memetic Computing*, **2**(1): 47–67, 2010, doi: 10.1007/s12293-009-0028-5.

19. T. Huang, X. Song, M. Liu, A Kriging-based non-probability interval optimization of loading path in T-shape tube hydroforming, *The International Journal of Advanced Manufacturing Technology*, **85**(5–8): 1615–1631, 2016, doi: 10.1007/s00170-015-8034-x.

20. L. Jiao, Y. Li, M. Gong, X. Zhang, Quantum-inspired immune clonal algorithm for global optimization, *IEEE Transactions on Systems, Man, and Cybernetics, Part B (Cybernetics)*, **38**(5): 1234–1253, 2008, doi: 10.1109/TSMCB.2008.927271.

21. W. Kuś, J. Dziatkiewicz, Multicriteria identification of parameters in microscale heat transfer, *International Journal of Numerical Methods for Heat & Fluid Flow*, **27**(3): 587–597, 2017, doi: 10.1109/TSMCB.2008.927271.

22. H.Y.K. Lau, V.W.K. Wong, An immunity approach to strategic behavioral control of intelligent transportation systems, *Engineering Applications of Artificial Intelligence*, **20**(3): 289–306, 2007, doi: 10.1016/j.engappai.2006.06.002.

23. H.Y.K. Lau, W.W.P. Tsang, A parallel immune optimization algorithm for numeric function optimization, *Evolutionary Intelligence*, **1**(3): 171–185, 2008, doi: 10.1007/s12065-008-0014-8.

24. Z. Lin, L.V. Zhigilei, V. Celli, Electron-phonon coupling and electron heat capacity of metals under conditions of strong electron-phonon nonequilibrium, *Physical Review B*, **77**: 075133-1–075133-17, 2008, doi: 10.1103/PhysRevB.77.075133.

25. E. Majchrzak, J. Dziatkiewicz, Second-order two-temperature model of heat transfer processes in a thin metal film subjected to an ultrashort laser pulse, *Archives of Mechanics*, **71**(4/5): 377–391, 2019, doi: 10.24423/aom.3131.

26. E. Majchrzak, J. Dziatkiewicz, Ł. Turchan, Analysis of thermal processes occurring in the microdomain subjected to the ultrashort laser pulse using the axisymmetric two-temperature model, *International Journal for Multiscale Computational Engineering*, **15**(5): 395–411, 2017.

27. E. Majchrzak, J. Dziatkiewicz, Ł. Turchan, Sensitivity analysis and inverse problems in microscale heat transfer, [in:] *Fluid Flow, Energy Transfer and Design II, Defect and Diffusion Forum*, vol. 362, pp. 209–223, Trans Tech Publications Ltd., 2015, doi: 10.4028/www.scientific.net/ddf.362.209.

28. A.S. Perelson, Applications of optimal control theory to immunology, [in:] *Recent Developments in Variable Structure Systems, Economics and Biology*, R.R. Mohler, A. Ruberti [Eds], vol. 162, pp. 272–287, Springer, New York, 1978, doi: 10.1007/978-3-642-45509-4_20.

29. A. Poteralski, Hybrid artificial immune strategy in identification and optimization of mechanical systems, *Journal of Computer Science*, **23**: 216–225, 2017, doi: 10.1016/j.jocs.2017.04.015.

30. A. Poteralski, M. Szczepanik, W. Beluch, T. Burczyński, Optimization of composite structures using bio-inspired methods, [in:] L. Rutkowski, M. Korytkowski, R. Scherer, R. Tadeusiewicz, L.A. Zadeh, J.M. Zurada [Eds], *Artificial Intelligence and Soft Computing, ICAISC 2014, Lecture Notes in Computer Science*, vol. 8468, pp. 385–395, 2014, doi: 10.1007/978-3-319-07176-3_34.

31. A. Poteralski, M. Szczepanik, R. Górski, T. Burczyński, Swarm and immune computing of dynamically loaded reinforced structures, [in:] L. Rutkowski, M. Korytkowski, R. Scherer,

R. Tadeusiewicz, L. Zadeh, J. Zurada [Eds], *International Conference on Artificial Intelligence and Soft Computing (ICAISC), Lecture Notes in Computer Science*, vol. 9120, pp. 483–494, Springer, Cham, 2015, doi: 10.1007/978-3-319-19369-4_43.

32. A. Poteralski, M. Szczepanik, J. Ptaszny, W. Kuś, T. Burczyński, Hybrid artificial immune system in identification of room acoustic properties, *Inverse Problems in Science and Engineering*, **21**(6): 957-967, 2013, doi: 10.1080/17415977.2013.788174.

33. A. Poteralski, M. Szczepanik, G. Dziatkiewicz, W. Kuś, T. Burczyński, Comparison between PSO and AIS on the basis of identification of material constants in piezoelectrics, [in:] L. Rutkowski, M. Korytkowski, R. Scherer, R. Tadeusiewicz, L.A. Zadeh, J.M. Zurada [Eds], *Artificial Intelligence and Soft Computing, ICAISC 2013, Lecture Notes in Computer Science,* vol. 7895, pp. 569–581, Springer, Berlin–Heidelberg, 2013, doi: 10.1007/978-3-642-38610-7_52.

34. A. Poteralski. G. Dziatkiewicz, Artificial immune system for effective properties optimization of magnetoelectric composites, *AIP Conference Proceedings*, **1922**(1): 140007-1–140007-10, 2018, doi: 10.1063/1.5019149.

35. J. Ptaszny, A. Poteralski, Optimization of porous structure effective elastic properties by the fast multipole boundary element method and an artificial immune system, [in:] *Proceedings of the 6th International Conference on Engineering Optimization,* Springer, 2018, doi: 10.1007/978-3-319-97773-7_88.

36. M. Szczepanik, A. Poteralski, A. Długosz, W. Kuś, T. Burczyński, Bio-inspired optimization of thermomechanical structures, [in:] L. Rutkowski, M. Korytkowski, R. Scherer, R. Tadeusiewicz, L.A. Zadeh, J.M. Zurada [Eds], *Artificial Intelligence and Soft Computing, ICAISC 2013, Lecture Notes in Computer Science*, vol. 7895, pp. 79–90, Springer, Berlin–Heidelberg, 2013, doi: 10.1007/978-3-642-38610-7_8.

37. S.T. Wierzchoń, *Artificial Immune Systems. Theory and Applications*, [in Polish: Sztuczne systemy immunologiczne. Teoria i zastosowania], Akademicka Oficyna Wydawnicza EXIT, Warszawa, 2001.

38. Z.M. Zhang, *Nano/Microscale Heat Transfer*, McGraw-Hill, 2007.

Received December 31, 2022; revised version February 5, 2023; accepted May 10, 2023.